

Drag models for Simulation Gas-Solid Flow in the Bubbling Fluidized Bed of FCC Particles

S. Benzarti, H. Mhiri, and H. Bournot

Abstract—In the current work, a numerical parametric study was performed in order to model the fluid mechanics in the riser of a bubbling fluidized bed (BFB). The gas-solid flow was simulated by mean of a multi-fluid Eulerian model incorporating the kinetic theory for solid particles. The bubbling fluidized bed was simulated two dimensionally by mean of a Computational Fluid Dynamic (CFD) commercial software package, Fluent. The effects of using different inter-phase drag function (the drag model of Gidaspow, Syamlal and O'Brien and the EMMS drag model) on the model predictions were evaluated and compared. The results showed that the drag models of Gidaspow and Syamlal and O'Brien overestimated the drag force for the FCC particles and predicted a greater bed expansion in comparison to the EMMS drag model.

Keywords—Bubbling fluidized bed, CFD, drag model, EMMS

I. INTRODUCTION

FLUIDIZED beds were widely used in industry during the last decades. They are characterized by their excellent solid mixing and their ability of higher heat transfer. Having achieved success in simulation of single phase flow, Computational Fluid Dynamics (CFD) is considered greatly promising for modeling multiphase flow. Nevertheless, CFD is still at the verification and validation stages for modeling multiphase flow, and more improvements regarding the flow dynamics and computational models are required to make it a standard tool in designing large scale industrial reactors.

There are two different classifications of CFD models in the literature for modeling gas-solid flow: The EULERIAN-LAGRANGIAN approach and the EULERIAN – EULERIAN approach. In the EULERIAN-LAGRANGIAN approach, the Newtonian equations of motion are solved for each individual particle. This approach also takes into account a collision model for commending the energy dissipation caused by the non ideal particle-particle interactions. The second approach, namely the Eulerian-Eulerian approach treats the different phases mathematically as continuous and fully interpenetrating.

S. Benzarti is with the National Engineering School of Monastir, Unit of Thermics and Thermodynamics of the Industrial Processes, Monastir, Tunisia (phone: 216-25-238-246; e-mail: salma_benzarti@yahoo.fr).

H. Mhiri is with the National Engineering School of Monastir, Unit of Thermics and Thermodynamics of the Industrial Processes, Monastir, Tunisia(phone: 216-98-45-16 ; e-mail: hatem.mhiri@enim.rnu.tn).

H. Bournot is with the IUSTI, UMR CNRS 6595, Technopôle Château-Gombert 5 rue Enrico Fermi 13013 Marseille.

Conservations equations (momentum, mass, energy balance) are derived to obtain a set of equations that have similar structure for all phases. To close the equations' system and to describe the rheology of the solid phase, constitutive equations are necessary.

The Kinetic Theory of Granular Flow (KTGF) has become a very promising tool for modeling gas-particle fluidized bed. Numerous studies on the hydrodynamic of gas-solid fluidized bed incorporating the KTGF have shown of this theory's efficiency in modeling bubbling fluidized bed. This studies were conducted by, Sinclair and Jackson [1], Ding and Gidaspow [2], Gidaspow [3], Benyahia et al [4], Pain et al [5], Taghipour et al [6], Johansson et al [7], Ehsan et al [8], etc

The interphase momentum transfer between the two phases represented by the drag force, play an important role in any multiphase flow approach. Due to its high relevance, this phenomenon was frequently investigated in the literature. The ultimate goal of these works was to get an optimum drag model for better fluidized bed hydrodynamics.

Zimmermann et al [9], reported that the original forms of Gidaspow and Syamlal O'brien are not applicable for modeling a small fluid catalytic cracking (Geldart A). F.taghipour et al [6] applied a two dimensional CFD technique to the fluidized bed of glass beads classified as Geldart B particles in order to investigate the momentum exchange between the gas and solids phases. Several drag models included in Fluent are used (the Syamlal and O'Brien drag model, the model developed by Gidaspow and that of Wen and Yu). The comparison of the model predictions with the experimental measurements in terms of the time average bed, pressure drop, bed expansion, and qualitative gas-solid flow pattern, gave a satisfying agreement for most operating conditions. Farshid Vejjhati et al [10], investigated a two dimensional multifluid Eulerian CFD model to investigate the effect of using different drag models in simulation of bubbling fluidized bed. They proposed to adjust the Di Felice drag model based up on the minimum fluidization conditions of the experimental data. The results showed that the adjusted Di Felice model reproduces well the experimental measurements. The models of Farshid Vejjhati et al [10] were upgraded by Ehsan Esmaili et al [8] to become suitable to the three dimensional version of the handled configuration. Similar results were found. Benjapon et al [11], applied a two and three dimensional CFD technique to the fluidized bed of FCC particles. The EMMS interphase exchange coefficient pioneered by Yang et al [12], was applied and developed. The results showed that the modified EMMS interphase exchange

coefficient can be used to reproduce the experimental measurement of FCC particles in a bubbling fluidized bed system with an appropriate scale factor.

In addition to the drag force, the coefficient of restitution can also affect the hydrodynamics of a fluidized bed. The effect of this coefficient was evaluated by F.Taghipour et al [6] in a 2D multifluid Eulerian CFD model over the hydrodynamics of a dense gas-solid fluidized bed. It was found that to model efficiently the bed dynamics with fundamental hydrodynamics models, the energy dissipation generated by the non ideal particle-particle interaction, has to be taken into consideration.

Further parameters may affect the simulation results of a bubbling fluidized bed, such as the wall boundary conditions. Li et al [13] investigated the impact of this parameter in a 2D simulation of a bubbling fluidized bed, for gas and solid phases, over the generated flow hydrodynamics. According to their investigation, Li et al [13] showed that the wall boundary conditions need to be specified with great care due to their high relevance over the hydrodynamics.

In the present work, a multifluid Eulerian Computational Fluid Dynamics model incorporating the Kinetic Theory of granular flow is considered in order to simulate the hydrodynamics of 2D gas-solid fluidized bed. The CFD simulations were carried out using a commercial software package, Fluent. These simulations allowed investigating and comparing the effect of different inter-phase drag functions (the drag model of Gidaspow [3], Syamlal and O'Brien [14] and the EMMS drag model [12]) over the model predictions.

II. COMPUTATIONAL FLUID DYNAMICS SIMULATION SET UP

We propose in the current work to solve the governing equations of mass, momentum and energy, by means of a multifluid Eulerian model incorporating the Kinetic Theory of Granular Flow (KTGF) available in the Computational Fluid Dynamics code, Fluent. A brief summary of the hydrodynamic model equations is reported below.

A. Conservation equations

1. Mass conservation equations

The conservation of mass for both phases can be written as:

$$\frac{\partial(\epsilon_g \rho_g)}{\partial t} + \nabla \cdot (\epsilon_g \rho_g \mathbf{u}_g) = 0 \quad (1)$$

$$\frac{\partial(\epsilon_s \rho_s)}{\partial t} + \nabla \cdot (\epsilon_s \rho_s \mathbf{u}_s) = 0 \quad (2)$$

The volume fractions are related as:

$$\epsilon_s + \epsilon_g = 1$$

2. Momentum conservation equations

The momentum conservation equations are described by:

$$\frac{\partial(\epsilon_g \rho_g \mathbf{u}_g)}{\partial t} + \nabla \cdot (\epsilon_g \rho_g \mathbf{u}_g \mathbf{u}_g) = \nabla \cdot (\boldsymbol{\tau}_g) - \epsilon_g \nabla P - \beta (\mathbf{u}_g - \mathbf{u}_s) + \epsilon_g \rho_g \mathbf{g} \quad (3)$$

$$\frac{\partial(\epsilon_s \rho_s \mathbf{u}_s)}{\partial t} + \nabla \cdot (\epsilon_s \rho_s \mathbf{u}_s \mathbf{u}_s) = \nabla \cdot (\boldsymbol{\tau}_s) - \epsilon_s \nabla P - \nabla P_s + \beta (\mathbf{u}_g - \mathbf{u}_s) + \epsilon_s \rho_s \mathbf{g} \quad (4)$$

The momentum exchange coefficient who represents the drag force between the phases is modeled in the current work as proposed by Gidaspow [3], Syamlal & O'Brien [14], and

the Energy Minimization Multi-Scale (EMMS) interphase exchange coefficient model, pioneered by Yang et al [12] are provided as follow:

3. Gidaspow drag function

To cover the whole range of void fraction Gidaspow [3] proposed to combine the Wen-Yu [15] and Ergun [16] equations. We define the voidage as the volume fraction of the gas phase. For a voidage greater than 0.8, the Wen-Yu equation was used. For a voidage less than 0.8 the Ergun equation was used.

$$\text{For } \epsilon_g \leq 0.8, \quad \beta = 150 \frac{(1-\epsilon_g)^2}{\epsilon_g} \frac{\mu_g}{(d_p)^2} + 1.75 (1-\epsilon_g) \frac{\rho_g}{d_p} |\mathbf{u}_g - \mathbf{u}_s| \quad (5)$$

$$\text{For } \epsilon_g > 0.8, \quad \beta = \frac{3}{4} C_d \frac{\epsilon_g (1-\epsilon_g)}{d_p} \rho_g |\mathbf{u}_g - \mathbf{u}_s| \epsilon_g^{-2.65} \quad (6)$$

Where

$$C_d = \begin{cases} \frac{24}{\text{Re}_s} [1 + 0.15 (\text{Re}_s)^{0.687}] & , \text{Re}_s < 1000 \\ 0.44 & , \text{Re}_s > 1000 \end{cases} \quad (7)$$

$$\quad (8)$$

The particle Reynolds number is given by:

$$\text{Re}_p = \frac{\epsilon_g \rho_g |\mathbf{u}_g - \mathbf{u}_s| d_p}{\mu_g} \quad (9)$$

4. Syamlal & O'Brien drag function

The Syamlal & O'Brien drag function is given by:

$$\beta = \frac{3}{4} \frac{\epsilon_s \epsilon_g \rho_g}{v_{rs}^2 d_p} C_D \left(\frac{\text{Re}_s}{v_{rs}} \right) |\mathbf{u}_s - \mathbf{u}_g| \quad (10)$$

Where

$$C_D = \left(0.63 + \frac{4.8}{\sqrt{\text{Re}_s / v_{rs}}} \right)^2 \quad (11)$$

And

$$v_{rs} = 0.5 \left(A - 0.06 \text{Re}_s + \sqrt{(0.06 \text{Re}_s)^2 + 0.12 \text{Re}_s (2B - A) + A^2} \right) \quad (12)$$

With

$$A = \epsilon_g^{4.14}, \quad B = 0.8 \epsilon_g^{1.28} \quad \text{for } \epsilon_g \leq 0.85 \quad (13)$$

Or

$$A = \epsilon_g^{4.14}, \quad B = \epsilon_g^{2.65} \quad \text{for } \epsilon_g > 0.85 \quad (14)$$

5. EMMS drag function

The EMMS interphase exchange coefficient model is expressed as follows:

$$\text{For } \epsilon_g \leq 0.74, \quad \beta = 150 \frac{(1-\epsilon_g)^2}{\epsilon_g d_p^2} \mu_g + 1.75 \frac{(1-\epsilon_g) \rho_g}{d_p} |\mathbf{u}_g - \mathbf{u}_s| \quad (15)$$

$$\text{For } \epsilon_g > 0.74, \quad \beta = \frac{3}{4} \frac{(1-\epsilon_g) \epsilon_g}{d_p} \rho_g |\mathbf{u}_g - \mathbf{u}_s| C_{D0} \omega(\epsilon) \quad (16)$$

With

$$\text{When } 0.74 \leq \epsilon_g \leq 0.82, \quad \omega(\epsilon) = -0.5760 + \frac{0.0214}{4(\epsilon_g - 0.7463)^2 + 0.0044} \quad (17)$$

When $0.82 \leq \varepsilon_g \leq 0.97$,

$$\omega(\varepsilon_g) = -0.0101 + \frac{0.0038}{4(\varepsilon_g - 0.7789)^2 + 0.0040} \quad (18)$$

When $\varepsilon_g > 0.97$,

$$\omega(\varepsilon_g) = -31.8295 + 32.8295\varepsilon_g$$

And

$$C_{D0} = \begin{cases} \frac{24}{\text{Re}_s} [1 + 0.15 (\text{Re}_s)^{0.687}] & , \text{Re}_s < 1000 \\ 0.44 & , \text{Re}_s > 1000 \end{cases} \quad (19)$$

$$, \text{Re}_s > 1000 \quad (20)$$

The particle Reynolds number is given by:

$$\text{Re}_s = \frac{\varepsilon_g \rho_g |u_g - u_s| d_p}{\mu_g}$$

The EMMS interphase exchange coefficient model was implemented into Fluent with User Defined Functions (UDF).

B. Kinetic Theory of Granular Flow

To close the solid phase momentum equations, the solid phase stresses should be described. The effective stresses in the solid phase resulting from direct collision and particle streaming can be described by the kinetic theory concepts. These concepts are used when the granular motion is dominated by collisional interactions. With analogy to thermodynamic temperature for gases, the handled model introduces a granular temperature that describes the solid velocity fluctuations. The granular temperature is defined as:

$$\Theta = \frac{1}{3} u'^2 \quad (21)$$

The solid phase transport equation for the granular temperature so-called granular temperature equation can be written as:

$$\frac{3}{2} \left(\frac{\partial(\varepsilon_s \rho_s \Theta)}{\partial t} + \nabla \cdot (\varepsilon_s \rho_s u_s \Theta) \right) = (-P_s I + \tau_s) : \nabla u_s - \nabla \cdot q - \gamma - J \quad (22)$$

In words this equation can be explained as:

The net change of fluctuating energy = the generation of fluctuating energy due to the local acceleration of the particles + the diffusion of the fluctuating energy + the dissipation of the fluctuating energy due to inelastic particle-particle collisions + the exchange of the fluctuating energy between gas and solid phase

To solve the complete granular temperature equation, Syamlal et al [17] proposed an algebraic form to this equation. They assumed that the granular energy is in a steady state and dissipates locally, thus convection and diffusion terms can be neglected. Considering only the dissipation and the generation terms, the algebraic form of the granular temperature is given

by:

$$0 = (-P_s I + \tau_s) : \nabla u_s - \gamma \quad (23)$$

C. Constitutive equations

1. The stress tensor

The stress tensor is modeled using the Newtonian stress-strain for each phase.

The stress tensor for the gas phase is given as:

$$\tau_g = -\varepsilon_g \left[\left(\xi_g - \frac{2}{3} \mu_g \right) (\nabla \cdot u_g) I + \mu_g ((\nabla u_g) + (\nabla u_g)^T) \right] \quad (24)$$

Where ξ_g is the bulk viscosity, is generally set to zero.

The stress tensor for the solid phase the stress tensor is:

$$\tau_s = -\varepsilon_s \left[\left(\xi_s - \frac{2}{3} \mu_s \right) (\nabla \cdot u_s) I + \mu_s ((\nabla u_s) + (\nabla u_s)^T) \right] \quad (25)$$

2. Solid pressure

The solid pressure which represents the normal solid phase forces due to particle-particle interactions is made up of two terms: a kinetic term and a collisional term as given by Lun et al [18]. It can be described by:

$$P_{s,KTGF} = \varepsilon_s \rho_s \Theta + 2 g_0 \varepsilon_s^2 \rho_s \Theta (1 + e) \quad (26)$$

3. Radial distribution function

The radial distribution function g_0 is a function that modifies the probability of collisions between particles.

$$g_0 = \left[1 - \left(\frac{\varepsilon_s}{\varepsilon_{s,max}} \right)^{1/3} \right]^{-1} \quad (27)$$

4. Solid bulk viscosity

The resistance of the particle suspension against expansion and compression is described by the solid bulk viscosity. That is generally described by the expression proposed by Lun et al [18] is often used.

$$\xi_s = \frac{4}{3} \varepsilon_s \rho_s d_p g_0 (1 + e) \sqrt{\frac{\Theta}{\pi}} \quad (28)$$

5. Solid shear viscosity

The tangential force which is due to the collisional and translational interactions of particles is represented by the solid shear viscosity. It is written as a sum of collisional and kinetic part:

$$\mu_{s,KTGF} = \mu_{s,col} + \mu_{s,kin} \quad (29)$$

In the current work, we adopted the model given by Gidaspow [3] and described as:

$$\mu_{s,col} = \frac{4}{5} \varepsilon_s \rho_s d_p g_0 (1 + e) \sqrt{\frac{\Theta}{\pi}} \quad (30)$$

$$\mu_{s,kin} = \frac{10}{96} \sqrt{\Theta \pi} \frac{\rho_s d_p}{(1 + e) \varepsilon_s g_0} \left[1 + \frac{4}{5} g_0 \varepsilon_s (1 + e) \right]^2 \quad (31)$$

6. Frictional model

For the frictional shear viscosity, we used the Schaeffer [19] model:

$$\mu_{s,f} = \frac{P_s \sin \phi}{2 \sqrt{I_{2D}}} \quad (32)$$

The conductivity of the solid fluctuating kinetic energy describes the diffusion of the granular energy as:

$$\kappa_s = \frac{150\rho_s d_p \sqrt{\Theta\pi}}{384(1+e)g_0} \left[1 + \frac{6}{5}\varepsilon_s g_0 (1+e) \right]^2 + 2\rho_s \varepsilon_s^2 d_p (1+e)g_0 \sqrt{\frac{\Theta}{\pi}} \quad (33)$$

The collisional dissipation of the solid fluctuating kinetic energy represents the rate of energy dissipation within the solid phase due to collisions between solid particles:

$$\gamma_s = 3(1-e^2)\varepsilon_s^2 \rho_s g_0 \Theta \left(\frac{4}{d_p} \sqrt{\frac{\Theta}{\pi}} \right) \quad (34)$$

III. NUMERICAL SIMULATION PROCEDURE AND BOUNDARY CONDITIONS

A. Bed geometry and simulation parameters

The experimental set up described by Benjapon et al [12] is used in this study in order to allow a direct comparison with experimental measurements. In their experiments, Benjapon et al [12] considered a pseudo 2D bed with 1.28 m in height, 0.3m in width and 0.05 m thickness. The solid bed was the FCC catalyst at a density of 1654 kg/m³ and a mean diameter of 75 μm were fluidized with air at ambient conditions. The static bed height is 0.24 m with solid volume fraction of 0.5. The two dimensional 2D geometry was performed and the eulerian multiphase model was used. The 2D computational domain was discretized using a uniform quadratic mesh with 4400 cells. Both the shape of the column and the computational domain are schematically displayed in Fig 1.

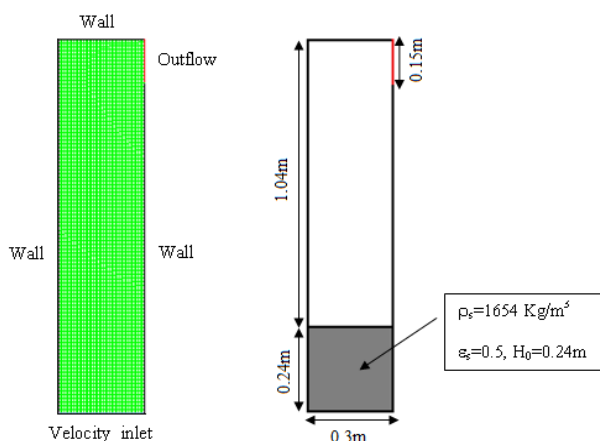


Fig. 1 (a) Schematic drawing and (b) Computational domain with the boundary conditions of a bubbling fluidized bed

Transient CFD simulations were carried out with a time step of 10⁻³ s and convergence criteria of 10⁻³ for each scaled residual component. The first order upwind scheme was employed for the spatial discretization of the continuity and the momentum equations while time was discretized using first order implicit. To solve the governing equations of mass and momentum conservation as well as the granular temperature equation, we used the method of finite volume. This method uses the phase-coupled SIMPLE called PC-SIMPLE algorithm, which is an extension of the SIMPLE algorithm to multiphase flows. The simulation parameters

used for the CFD simulation of the 2D fluidized bed are shown in Table I.

TABLE I
SIMULATION AND MODEL PARAMETERS

Description	Value	Comment
Bed height H	1.28m	Fixed value
Bed width	0.3m	Fixed value
Static bed height H ₀	0.24m	Fixed value
Grid resolution	44×100	Specified
Gas density ρ _g	1.2Kg/m ³	Air
Particle density ρ _s	1654 Kg/m ³	FCC
Particle diameter d _s	75μm	Uniform distribution
Initial solid volum fraction ε ₀	0.5	Fixed value
Angle of internal friction	30°	Fixed value
Restitution coefficient	0.7	Fixed value
Specularity coefficient	0.0001	Fixed value
Maximum particle packing limit	0.64	Fixed value
Time step	10 ⁻³ s	Specified

B. Boundary conditions

The computational geometry used for the simulation consisted of a bottom gas inlet with a non uniform parabolic velocity profile, an outflow boundary condition on top with a fully developed gas flow. At the wall, the no slip boundary condition was used for the gas phase.

For the solid phase the partial slip boundary condition developed by Johnson and Jackson (1987) was assumed with a specularity coefficient of 0.0001.

IV. RESULTS AND DISCUSSION

A. Drag model comparison

To get an optimum drag model for better fluidized bed hydrodynamics, the classical drag model available in Fluent 6.2 of Gidaspow [3], Syamlal & O'Brien [14] and the EMMS drag models were investigated.

The simulations were performed for 15 s of real flow time to allow for complete fluidization. The 2D results were time-averaged over a period of 10 s.

Fig 2 depicts the flow structure of the bed simulated by the Gidaspow drag model. The simulations results show an overestimation of the fluidization, after 8 s, the conditions are more characteristic of a fast fluidization.

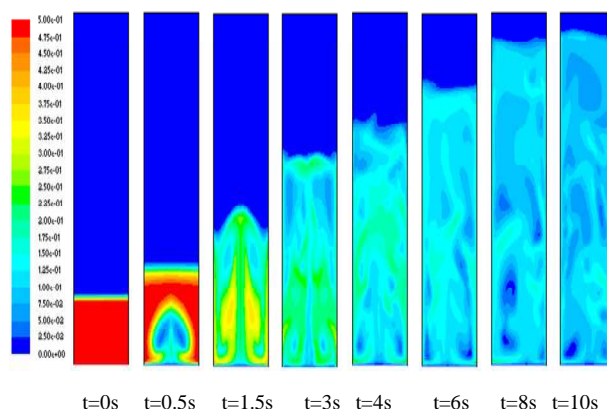


Fig. 2 Contour plots of the solid volume fraction with Gidaspow drag model

The contour plot of solid fraction for the Syamlal and O'Brien drag model with the same operating conditions are shown in Fig 3. The flow pattern is similar to that obtained with the Gidaspow drag model. Similar overestimations were observed by other researchers (McKeen and Pugsley [20], Zimmermann and Taghipour [9], Peng Li et al [21]).

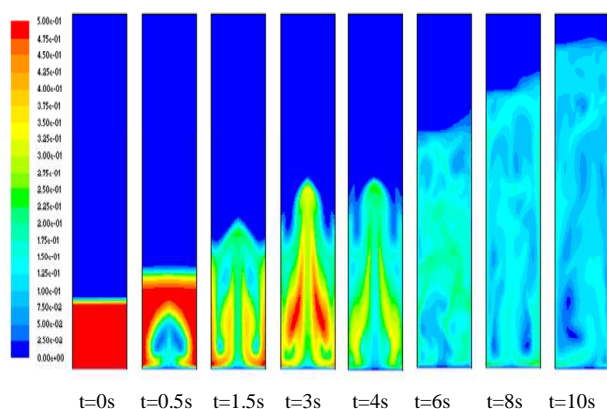


Fig. 3 Contour plots of the solid volume fraction with Syamlal & O'Brien drag model

In Fig 4, the axial profile of the solid volume fraction versus the system height for the three models (Gidaspow, Syamlal & O'Brien and EMMS drag model) is displayed. Gidaspow and Syamlal & O'Brien show that there is no formation of the dense bottom zone which characterize the bubbling fluidized bed. Hence, neither of these models can be applied, in its original form to a fluidized bed containing FCC particles of 75 μm diameter.

The axial profile of the solid volume fraction versus the system height for the EMMS interphase exchange coefficient model shows a consistent increase in the bed height and the formation of a dense bottom zone. These results support that to predict the results of FCC particles in a bubbling fluidized bed with 75 μm diameter, the EMMS drag model can be used.

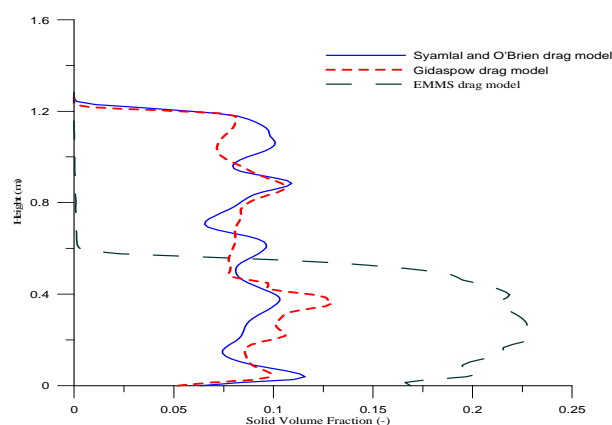


Fig. 4 The time-averaged solid volume fraction versus the system height with classical drag model

B. Radial solid volume fraction profile

Fig 5, displays the average radial solid volume fraction at different bed heights for the EMMS interphase exchange

coefficient model. It can be found that increasing the bed height reduce the solid volume fraction at the wall decreases. The solid volume fraction shows higher near the wall whilst accumulating more particles from the core. This is due to the wall effect on the gas-solid flow.

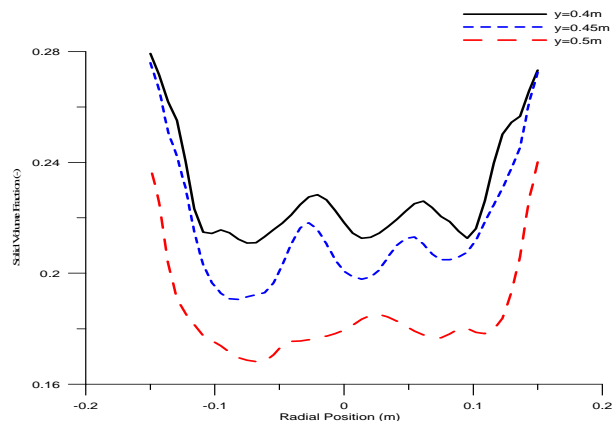


Fig. 5 Radial Solid Volume Fraction at different bed heights

C. Particle velocity profile

The radial profile of vertical solid velocities at different bed heights is plotted in Fig 6. It can be seen that the time mean solid velocity is downward near the wall region and is upward in the core region. Such flow patterns are associated to the formation, motion and split of bubbles. Bubbles entraining particles with them move up in the center of the fluidized bed. When arriving at the fluidized-bed surface, bubbles breakup and release the particles within them. Particles then fall downward along the wall.

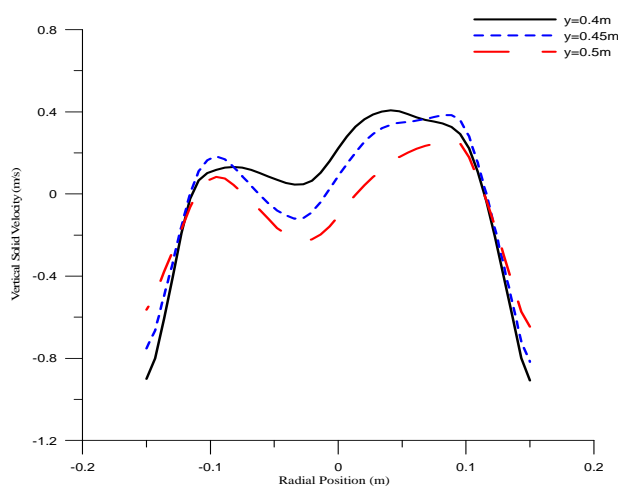


Fig. 6 Radial profile of vertical solid velocities at different bed heights

V. CONCLUSION

An Eulerian-Eulerian CFD model incorporating the kinetic theory of granular flow was applied using commercial CFD package Fluent v 6.2 in order to study the hydrodynamics' characteristics inside a bubbling fluidized bed of FCC

particles. Three drag models include those of Syamlal & O'Brien, Gidaspow available in Fluent and the EMMS interphase exchange coefficient implemented into Fluent with User Defined Functions (UDF). Once used, the corresponding results were compared. The ultimate goal of this work was to get an optimum drag model for better fluidized bed hydrodynamics. The simulation results showed that the drag models of Gidaspow and Syamlal & O'Brien highly overestimate the gas-solid drag force for the FCC particles and could not predict the formation of dense phase in the fluidized bed. On the other hand, the EMMS interphase exchange coefficient shows a consistent increase in the bed height and the formation of a dense bottom zone. These results supports that to predict the results of FCC particles in a bubbling fluidized bed with 75 μm diameter, the EMMS drag model can be used. The solid volume fraction profile at three heights within the riser shows higher values near the wall whilst accumulating more particles from the core.

TABLE II
NOMENCLATURE

Symbol	Quantity
C_{D0}	Drag coefficient (–)
d_p	Particle diameter (m)
e	Restitution coefficient between solids or particles (–)
e_w	Restitution coefficient between particle and wall (–)
g	Gravity force (m/s^2)
g_0	Radial distribution function (–)
H	Height of system (m)
H_0	Height of initial solid bed (m)
I	Unit tensor (–)
J	Granular energy transfer ($\text{kg/m}^3\text{s}^3$)
I_{2D}	Second invariant of the deviator of the rate of strain tensor (Pa)
P	Pressure (kPa)
q	Diffusion of fluctuating energy (kg/s^3)
Re	Reynolds number (–)
t	Time (s)
u	Velocity (m/s)
Greek letters	
β	Interphase exchange coefficient ($\text{kg/m}^3\text{s}$)
ε	Volume fraction (–)
γ	Dissipation of fluctuating energy ($\text{kg/m}^3\text{s}^3$)
Θ	Granular temperature (m^2/s^2)
μ	Shear viscosity (Pa.s)
ζ	Bulk viscosity (Pa.s)
ρ	Density (kg/m^3)
τ	Shear stress tensor (N/m^2)
ϕ	Angle of internal friction (°)

REFERENCES

- [1] Sinclair JL, Jackson R, "Gas-particle flow in a vertical pipe with particle-particle interactions," *AIChE J.*, vol.35, pp.1473–1496, 1989.
- [2] J. Ding, D. Gidaspow, "A bubbling model using kinetic theory of granular flow," *AIChE J.*, vol. 36, pp.523–538, 1990.
- [3] D. Gidaspow, "Multiphase Flow Fluidization: Continuum Kinetic Theory Description," in Academic Press, Boston, 1994.
- [4] Benyahia, S., Arastoopour, H., Knowlton, T., Massah, and H., "Simulation of particles and gas flow behavior in the riser section of a circulating fluidized bed using the kinetic theory approach for the particulate phase," *Powder Technology J.*, vol.112 pp.24–33. 2000.
- [5] Pain, C., Mansoorzadeh, S., Oliveira, C. R. E. D. and Goddard, A. J. H., "Numerical Modeling of Gas-Solid Fluidized Beds Using the Two-Fluid

Approach," *International Journal for Numerical Methods in Fluids*, vol.36, pp.91–124, 2001.

- [6] Taghipour F, Ellis N, and Wong C, "Experimental and Computational Study of Gas-Solid Fluidized Bed hydrodynamics," *Chemical Engineering Science J.*, vol. 60, no.24, pp.6857–6867, 2005.
- [7] Johansson, K., van Wachem, B.G.M., Almstedt, A.E., "Experimental validation of CFD models for fluidized beds: Influence of particle stress models, gas phase compressibility and air in flow models," *Chemical Engineering Science J.*, vol. 61, pp.1705–1717, 2006.
- [8] Ehsan Esmaili, Nader Mahinpey, "Adjustment of drag coefficient correlations in three dimensional CFD simulation of gas–solid bubbling fluidized bed," *Advances in Engineering Software J.*, vol.42, pp.375–386, 2011.
- [9] Zimmermann, S. and F. Taghipour, "CFD Modeling of the Hydrodynamics and Reaction Kinetics of FCC Fluidized Bed Reactors," *Ind Eng Chem J.*, vol.44, pp.9818–9827, 2005.
- [10] Farshid Vejjahati, Nader Mahinpey, Naoko Ellis and Mehrdokht B. Nikoo, "CFD Simulation of Gas–Solid Bubbling Fluidized Bed: A New Method for Adjusting Drag Law," *Can. J. Chem. Eng.*, vol. 87, pp.19–30, 2009.
- [11] Benjapon Chalermsinsuwana, Dimitri Gidaspow, and Pornpote Piumsomboon, "Two- and three-dimensional CFD modeling of Geldart A particles in a thin bubbling fluidized bed: Comparison of turbulence and dispersion coefficients," *Chemical Engineering J.*, vol.171, pp.301–313, 2011.
- [12] N. Yang, W. Wang, W. Ge, J. Li, "CFD simulation of concurrent-up gas-solid flow in circulating fluidized beds with structure-dependent drag coefficient," *Chem. Eng. J.*, vol. 96, pp.71–80, 2003.
- [13] Tingwen Li, John Grace, and Xiaotao Bi, "Study of wall boundary condition in numerical simulations of bubbling fluidized beds," *Powder Technology J.*, vol.203, pp. 447–457, 2010.
- [14] Syamlal, M., and O'Brien, T. J., "Computer simulation of bubbles in a fluidized bed," *AIChE Symposium Series*, vol. 85, pp.22–31. 1989.
- [15] Wen, C. Y., & Yu, Y. H. "Mechanics of fluidization, Chemical," *Engineering Progress Symposium Series*, vol.62, pp.100–111. 1966.
- [16] Ergun S., "Fluid flow through packed columns," *Chem Eng Progr* vol.48, pp.89–94. 1952.
- [17] O'Brien TJ, Syamlal M, "Particle cluster effects in the numerical simulation of a circulating fluidized bed," *In Preprint Volume for CFB-IV. Avidan AA, ed. AIChE; New York*, pp.430–435. 1993.
- [18] Lun, C. K. K., S. B. Savage, D. J. Jeffrey and N. Chepurmy, "Kinetic Theories for Granular Flow: Inelastic Particles in Couette Flow and Slightly Inelastic Particles in a General Flow Field," *Fluid Mech. J* vol.140, pp.223–256. 1984.
- [19] Schaeffer D. G., "Instability in the Evolution Equations Describing Incompressible Granular Flow," *Journal of Differential Equations*, Vol.66, no.1, pp.19–50. 1987.
- [20] McKeen, T., & Pugsley, T. "Simulation and experimental validation of a freely bubbling bed of FCC catalyst," *Powder Technology*, vol.129, pp. 139–152. 2003.
- [21] Peng Li, Xingying Lan, Chunming Xu, Gang Wang, Chunxi Lu, Jinsen Gao, "Drag models for simulating gas–solid flow in the turbulent fluidization of FCC particles," *Particology J.*, vol.7, pp.269–277, 2009.